Chemical Engineering Research and Design 202 (2024) 468–479

Contents lists available at ScienceDirect

Chemical Engineering Research and Design

journal homepage: www.elsevier.com/locate/cherd

Flux decline in crossflow ultrafiltration-based diafiltration process for lignin recovery from a deep eutectic solvent comprised of lactic acid and choline chloride

Mahsa Gholami [a], Bram Middelkamp [a], Yagnaseni Roy [a,b], Wiebe M. de Vos [c], Boelo Schuur [a,*]

[a] University of Twente, Faculty of Science and Technology, Sustainable Process Technology, PO Box 217, 7500 AE Enschede, the Netherlands
[b] Indian Institute of Science (IISc), Centre for Sustainable Technologies, Bangalore 560012, India
[c] University of Twente, Faculty of Science and Technology, Membrane Science and Technology, PO Box 217, 7500 AE Enschede, the Netherlands

ARTICLE INFO

Keywords:
Ultrafiltration-Diafiltration
Crossflow
Deep eutectic solvent (DES)
Lignin recovery
Fouling
Modeling

ABSTRACT

This study investigates a continuous ultrafiltration (UF)-based diafiltration (DF) method to separate and purify lignin from a deep eutectic solvent (DES) containing lactic acid and choline chloride after biomass delignification. A crossflow setup with a polyether sulfone UF membrane with a molecular weight cut off of 5000 Da was used to evaluate flux decline and fouling in this process. Under different pressure, feed flowrate, lignin, and DES concentrations, lignin rejection is around 0.90. Higher lignin and DES concentrations increase filtration resistance, and thus decrease flux at constant pressure. On the basis of a previously setup model based on dead-end filtration, a modeling approach was further developed to predict the system size required to implement UF-DF on a large scale. The results shows that at a constant pressure, the membrane system's area increases as the cake layer thickness over the membrane's surface increases.

1. Introduction

After cellulose, lignin is the second most abundant complex organic material in the world and it has a great potential to act as a future source for biofuels and valuable chemicals (Arni, 2018; Chovau et al., 2013; Putro et al., 2016). Extracting and purifying lignin from wood without compromising cellulose quality is a challenging process. For instance, in the kraft process, a traditional method of making paper, lignin and hemicellulose are removed from cellulose using an aqueous solution of sodium hydroxide and sodium sulfide. This process removes lignin, which is then heavily sulfurized and frequently regarded as a waste product of low value. Less than 2% of the lignin is used to create higher-value chemicals, the majority is burned for heat and electricity. (Pérez et al., 2021) Over the past years, studies appeared on development of suitable extraction methods to recover lignin from black liquor (Morya et al., 2022), and on development of an alternative pulping processes, such as organosolv pulping. Organosolv pulping, and similar approaches have as benefit over kraft pulping that sulfur-free lignin may be recovered as a byproduct with beneficial application potential (Zijlstra et al., 2020). Recovering lignin and hemicellulose allows for complete valorization of the biomass, which is a step towards sustainable co-production of these plant-based materials (Putro et al., 2016).

Recently deep eutectic solvents (DES) have emerged as a promising solvent for the pulping of wood (Jablonsky et al., 2018; Li et al., 2017; Smink et al., 2019; Tan et al., 2020). DESs are mixtures of two or more components (Liu et al., 2021; Wang et al., 2022) that can form extensive hydrogen bonds with one another, forming a eutectic mixture. The melting points of DES mixtures decrease much more (>50 °C) than would be expected for ideal mixtures (Schuur et al., 2019). A pulping process using such a solvent can produce sulfur free and thus higher value lignin as a byproduct. Utilizing DESs in this process is comparable to organosolv, but has advantages over acid-based organosolv cooking, as certain DES constituents, such as halogen anions, can exhibit catalytic activity (da Costa Lopes et al., 2020; Smink et al., 2019).

Lignin valorization is thought to be simplified by employing a sustainable method that fractionates heterogeneous lignin (heterogeneity dependent on molecular weight) into numerous homogeneous fractions (Deuss et al., 2015; Pang et al., 2021; Sun et al., 2018; Xu et al., 2020). Extraction of lignin from the DES-based black liquor has been investigated, and several viable extraction methods have been explored, such as cold water precipitation (Holtz et al., 2020; Smink et al., 2020a), liquid-liquid extraction (LLX) (Gholami et al., 2023; Smink et al., 2020a, 2020b) and membrane separation (Gholami et al., 2022; Ippolitov et al.,

* Correspondence to: Drienerlolaan 5, Meander 221, 7522 KE, Enschede, the Netherlands.
E-mail address: b.schuur@utwente.nl (B. Schuur).

https://doi.org/10.1016/j.cherd.2024.01.013
Received 16 November 2023; Received in revised form 8 January 2024; Accepted 9 January 2024
Available online 12 January 2024

Nomenclature

J	Permeate flux, (m/s)
r	Lignin rejection, (−)
R_f	Filtration resistance due to pore-blocking, concentration polarization, and the cake-fouling layer, (m^{-1})
R_m	Clean membrane resistance, (m^{-1})
R_t	Total filtration resistance, (m^{-1})
R_{irr}	Initial irreversible resistance, (m^{-1})
K_1	Maximum thickness factor, $(m.L/g)$
K_2	Cake growth coefficient, (L/g)
K_3	Specific cake resistance, (m^{-2})
δ	Thickness of the cake layer, (m)
δ_{max}	Maximum thickness of the cake layer, (m)
$C_{0,DES}$	Initial DES concentration in the feed, (g/L)
C_0	Initial lignin concentration in the feed, (g/L)
C_p	Lignin concentration in the permeate, (g/L)
C_r	Lignin concentration in the retentate, (g/L)
V_r	Total volume flowrate in the retentate, (m^3/s)
u_{in}	Inlet feed velocity, (m/s)
ΔP	Transmembrane pressure, (Pa)
ΔP_{loss}	The hydraulic pressure drop along the feed channel, in the feed flow direction, (Pa)
f	Friction coefficient
l	Distance along the feed channel, (m)
a	Cell surface area, (m^2)
i	Coordinate along membrane channel, (m)
dt	Filtration time, (second)
u	Bulk velocity of flow in the feed channel, (m/s)
L	Length of the membrane module, (m)
W	width of the membrane module, (m)
h	Hydraulic diameter of the feed channel, (m); for a rectangular channel $(H \ll W)$, h= 2 H
H	Height of the feed channel, (m)

Greek symbols

ϑ	Kinematic viscosity, (m/s)
μ	Viscosity, $(Pa.s)$
ρ	Density, (kg/m^3)

Dimensionless parameters

Re	Reynolds number, $(\mathrm{Re} = \frac{uh}{\vartheta})$

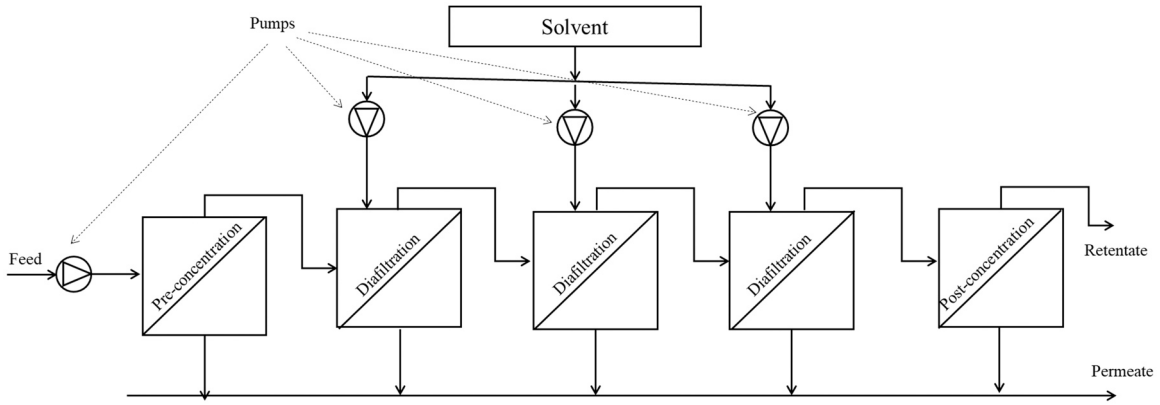

Fig. 1. Principle of continuous ultrafiltration-based diafiltration (UF-DF) as shown in the previous study (Gholami et al., 2022).

2022). Next to fractionation after DES-based pulping, also for other lignin separations, studies have discussed various types of ultrafiltration (UF) membranes for lignin separation and fractionation. These include separations from the effluents resulting from various lignocellulose biomass treatment processes (Fernández-Rodríguez et al., 2018; A. S. Jönsson et al., 2008; Toledano et al., 2010). This research builds on earlier study (Gholami et al., 2022), focused on developing a membrane-based separation technique for lignin recovery from DES-black liquor.

In order to obtain lignin as pure as possible from the effluent of a DES-based delignification process using an UF method, it is necessary to dilute the lignin-rich retentate with a suitable solvent to reduce the DES concentration. Ultrafiltration-based diafiltration (UF-DF) refers to the use of UF with a diluent solvent (Lipnizki, 2010; Madsen, 2001). UF-DF simulations such as the continuous flow process displayed in Fig. 1 (Gholami et al., 2022) can be developed using experimental data to parametrize the process in terms of rejection and pressure drop. Moreover, UF-DF can also be used in a batch mode (Stoner et al., 2004). For larger scale though, continuous processing is desired (Madsen, 2001).

The potential of UF-DF processes for purifying and concentrating dissolved lignin in black liquor following biomass delignification has been demonstrated (Servaes et al., 2017; Tanistra and Bodzek, 1998). However, in none of the previously cited studies the impact of membrane fouling and cake formation during the filtration process was studied. Membrane fouling is still one of the major challenges in membrane separation (Du et al., 2019; Li et al., 2020; Wang et al., 2020), and since our previous work only looked into batch processes (Gholami et al., 2022), additional research is needed in a crossflow UF module to study fouling and be able to forecast of the system's long-term operation. Practical parameters such as change in the flux permeation rate and, correspondingly, the system size necessary to continue the process over a relatively long operating time need to be determined.

In the previous study (Gholami et al., 2022), we used a stirred dead-end filtration setup to study the applicability of an UF-DF process for recovery of lignin dissolved in a DES-pulping stream comprising lactic acid and choline chloride after lignocellulose delignification. Employing experimental data on lignin fouling under varying feed concentrations and hydrodynamic flow conditions, a modeling approach was created to predict the system size and operating conditions necessary to implement the UF-DF process. In the current work, in order to gain a comprehensive understanding of flux decline, fouling, and lignin rejection under industrially-favorable crossflow conditions, a lab-scale crossflow setup was used. To reproducibly produce feed with varying percentages of DES and lignin, lignin was isolated from

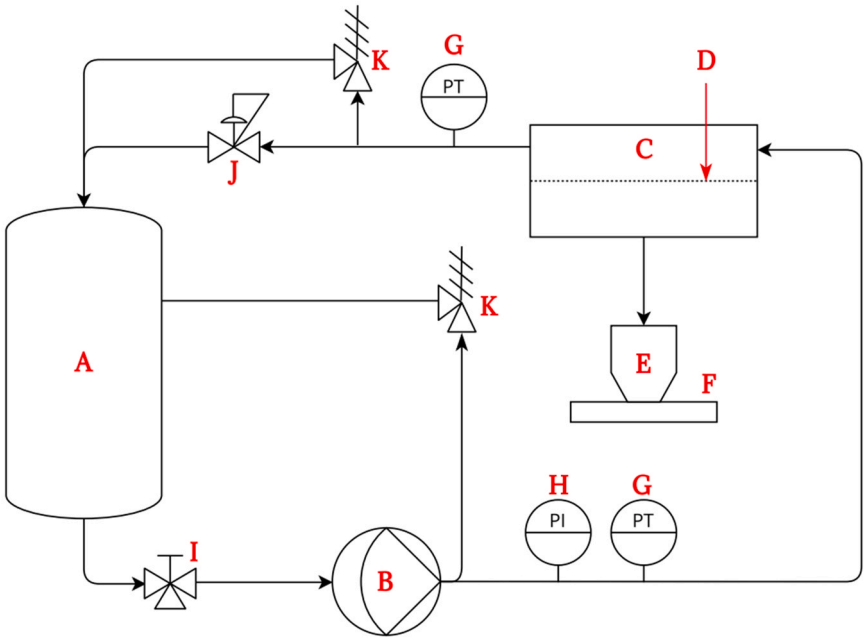

Fig. 2. Schematic diagram of the crossflow UF setup, used for the current work. (A) Feed vessel, (B) Diaphragm pump, (C) Membrane module, (D) Membrane, (E) Glass container to collect permeate, (F) weighing scale, (G) pressure transmitter, (H) pressure indicator, (I) drain valve, (J) back-pressure valve, and (K) pressure relief valve.

DES-black liquid following biomass delignification using cold water precipitation and recombined with DES consisting of lactic acid and choline chloride to the required concentration. The mixture was then diluted with a 70:30 (v:v) acetone-water mixture, due to the high solubility of lignin in this mixture (Domínguez-Robles et al., 2018), which can also be used as solvent for the separation of hemicellulose and its derivatives in a reverse osmosis process (Roy et al., 2023). To aid process development in minimizing fouling, the effects of membrane fouling were predicted using an modified version of the numerical simulation-based method used in prior work (Gholami et al., 2022). To accomplish this, the filtration flux for various feed concentrations and flowrates was evaluated and fitted to experimental data in order to obtain constant parameters of maximum thickness factor, cake growth coefficient, and specific cake resistance. Then, these parameters were utilized to forecast flux decline and filtration resistance in a large-scale UF-DF process.

2. Experimental technique and equipment

2.1. Chemicals used

A mixture of MilliQ water and technical grade acetone from Boomlab in The Netherlands was applied as solvent to dilute DES and DES-based solutions (DES-black liquor). The DES was prepared by mixing 90 wt% lactic acid in aqueous solution from VWR Chemicals and choline chloride (98 wt%) from Sigma Aldrich in a weight ratio of 10:1 (dry lactic acid to choline chloride). The DES-black liquor has been obtained at Center Technique du Papier (CTP) by delignification of spruce wood at 130 °C for 4 h, with DES to wood (spruce chips from Sappi Austria Produktions-GmbH & Co. KG.) ratio of 7 [g/g] and DES consisting of lactic acid and choline chloride with weight ratio of 10 to 1 [g/g]. MilliQ water was used for sample preparation and analysis.

2.2. Membrane used

Experiments were done using an ultrafiltration flat sheet membrane (GR90PP) from Alfa Laval with molecular weight cut off (MWCO) of 5000 Da. The membrane is polyethersulfone polymer based with polypropylene (PP) support material. The durability of membrane against solvent (acetone-water) has been checked in previous study, showed that the membrane is durable in this solvent (Gholami et al., 2022). By soaking the membranes overnight in MilliQ water, preservatives were removed prior to experimentation. To remove any residual preservatives, the membranes were flushed for 30 min at desired pressure and flowrate with MilliQ water.

2.3. Experimental setup

A schematic diagram of the crossflow UF setup used in this work is shown in the Fig. 2. The membrane setup consists of: (A) a stainless steel cylindrical feed vessel with a capacity of 15 L, (B) a diaphragm pump (Hydra Cell P200), (C) a membrane module (a detailed schematic of membrane module has been provided in the Supporting information (S1)), (D) UF membrane with the process area of 0.0037 m^2 (77 ×48 mm), (E) a closed-top glass container to collect solution permeate, (F) weighing scale (Kern DS8K0.05) with connection to the computer to read flux over time, (G) pressure transmitter, (H) pressure indicator, (I) drain valve, (J) back-pressure valve, and (K) pressure relief valve. To regulate the feed flowrate, the frequency of the pump can be varied. After the membrane module, a manually adjustable back pressure valve allows the system pressure to be set. Using pressure transmitters, the pressure is measured directly after the pump and after the membrane module. This allows the measurement of both transmembrane pressure (the permeate side was always at atmospheric pressure) and pressure drop across the membrane module and tubing. The pressure loss across the membrane cell and tubing remained below 0.1 bar, making it negligible for our measurements. In addition, a pressure gauge was added after the pump. Two safety loops were set up to guarantee that the pump can always circulate fluids. The permeate was collected continuously and weighed in a closed jar on a scale.

2.4. Chemical analysis

Chemical analysis of retentate, permeate, and feed samples was performed using an Agilent 1260 Infinity Gel Permeation Chromatography (GPC). The GPC machine was equipped with a UV detector

Table 1
Mathematical formulation for data analysis (Gholami et al., 2022).

Permeation flux (m/s)	$J = \frac{\Delta P}{\mu R_t}$	(2)
Total resistance (m^{-1})	$R_t = \frac{\Delta P}{\mu J} = R_m + R_f$	(3)
Lignin rejection (-)	$r = 1 - \frac{C_p}{C_r}$	(4)

running at 254 nm, a refractive index detector, and 3 GPC PLgel 3 m MIXED-E column in series. The column was operated at 40 °C and a 95:5 (v:v) tetrahydrofuran and water mixture as mobile phase. The mobile phase flowrate was kept at 1 mL/min. Apparent molecular weight distributions were based on calibrated distributions with polystyrene solutions having molecular weights ranging from 162 to 27,810 g/mol.

2.5. Experimental procedure

2.5.1. Feed preparation

Water and DES-black liquor were mixed at room temperature in mass ratios of water to DES-black liquor of 3.5:1 g/g and left over night at room temperature to precipitate lignin. The solid was then filtered out using a vacuum filtration, washed twice with 100 mL of water and dried overnight under pressure of 50 mbar. Water-precipitated lignin was combined with DES and a mixture of acetone-water (70:30 volume ratio) to produce lignin feed solutions ranging from 4.5 to 30 g/L. The apparent molecular weight distribution for the water-precipitated lignin used in this work is presented in the Supporting information S2. Overall the apparent molecular weight ranges from 200 to 20,000 g/mol, with an average of 3000 g/mol.

2.5.2. Crossflow membrane procedure

All experiments were carried out at 22 °C (± 2 °C) and filtration was carried out during 20 h. A new membrane sheet was used for each experiment, which was preliminary cleaned of preservatives using the method described in Section 2.2. For all experiments, before contacting the membranes with the feed solution, they were flushed for 30 min with the acetone-water (70:30 v:v) mixture used to make lignin feed solutions with at desired pressure and flowrate to evaluate the membrane resistance against solvent. This time (30 min) was set taking into account that membrane swelling will reach pseudo-equilibrium state in less than 30 min. Each experiment was repeated at least two times with different membrane samples but the same feed solutions.

The permeate flux was measured over time using the weighing scale and density of solution as described in Eq. 1:

$$J = \frac{1}{A}\frac{dM}{\rho dt} = \frac{1}{A}\frac{dV}{dt} \quad (1)$$

In this equation, A is active membrane area in m^2, M and V are permeated mass (kg) and permeated volume (m^3), respectively. The term

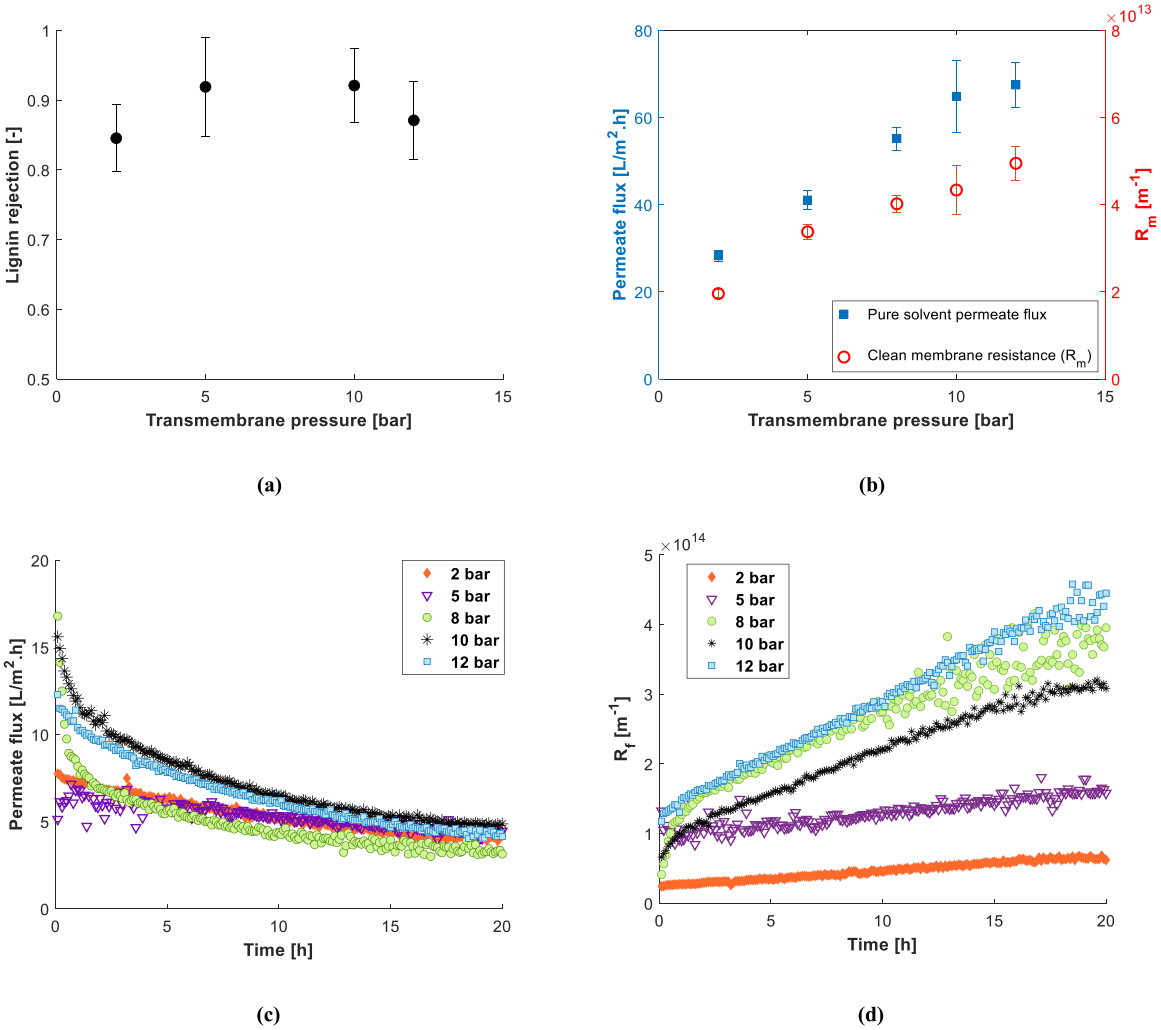

Fig. 3. Influence of different transmembrane pressure on: (a) lignin rejection, (b) pure solvent flux (acetone-water 70:30 v:v) and clean membrane resistance (c) flux decline and (d) filtration resistance, for a feed of 15 g/L lignin, 229 g/L DES in acetone-water (70:30 v:v) with a feed flowrate of 8.71 mL/s.

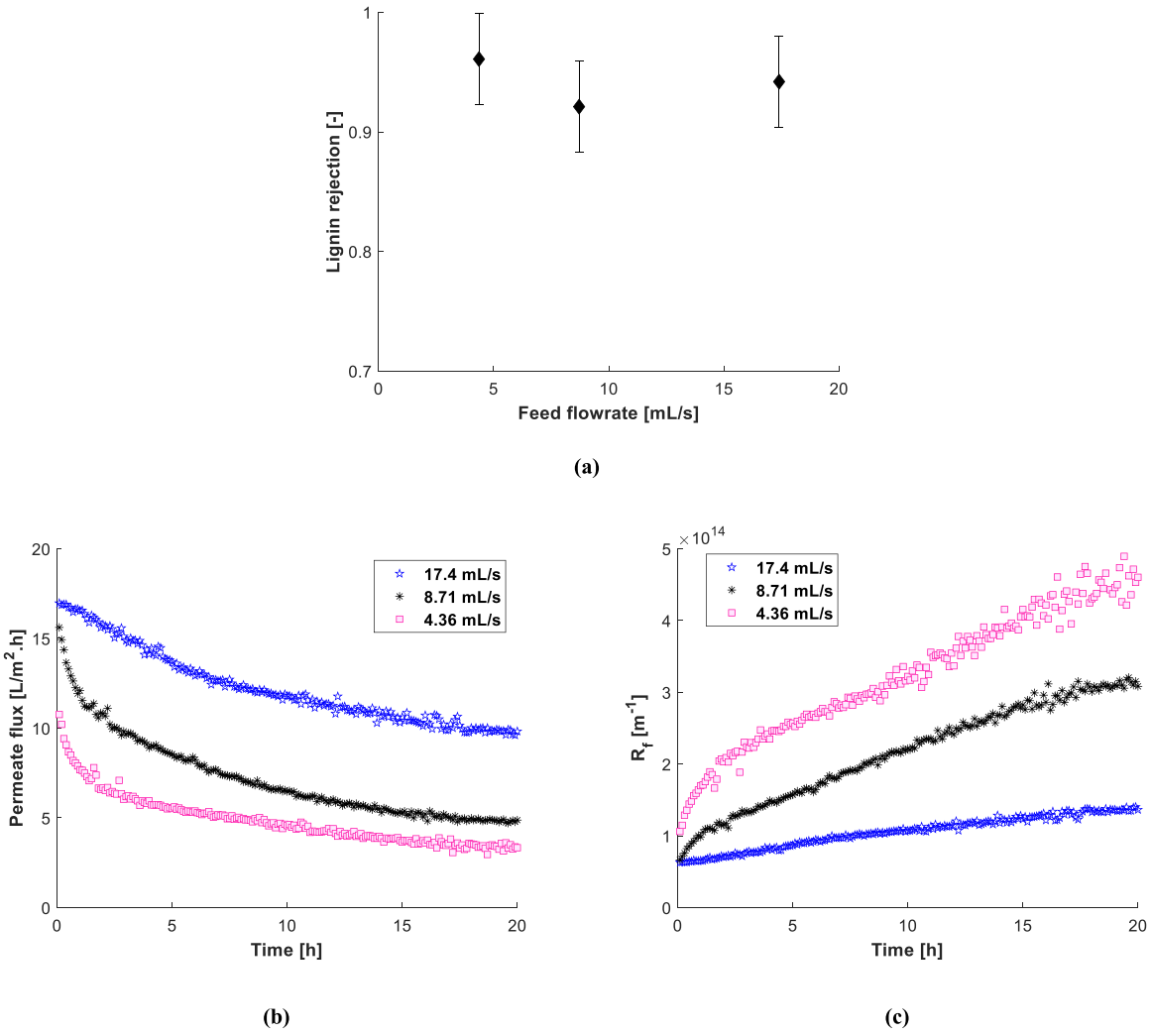

Fig. 4. Influence of feed flowrate on: (a) lignin rejection, (b) flux decline and (c) filtration resistance, for a feed of 15 g/L lignin, 229 g/L DES in acetone-water (70:30 v:v) under the transmembrane pressure of 10 bar. The clean membrane resistance, R_m, is $4.42 \times 10^{13} \pm 13.7\%$ (m^{-1}) for all trials.

ρ is the density of the permeated solution in (kg/m^3), and dt is the filtration time in seconds.

For each experimental trial, the permeation flux (J) was determined via Eq. 1. Subsequently, Eqs 2–4 presented in Table 1 were employed to calculate the t total resistance (R_t) and lignin rejection (r). These calculation procedures were thoroughly explained in the previous study. (Gholami et al., 2022) Densities and viscosities of feed, retentate and permeate also were taken from previous study (Gholami et al., 2022).

3. Results and discussion

To gain a better understanding of an UF-DF membrane system for lignin recovery from DES-black liquor, lignin rejection, flux decline, and filtration resistance during crossflow ultrafiltration were investigated under varied operational conditions and feed concentrations. For this, at the end of each experiment, the filtration resistance was determined using Eq 3. As indicated in section 2.5, the pure solvent flux (acetone-water (70:30 v:v)) at given pressure and feed flowrate was employed in Eq 2, to calculate the clean membrane resistance ($R_t = R_m$), for each experiment. For a pressure of 10 bar, the measured clean membrane resistance is $4.42 \times 10^{13} \pm 13.7\%$ (m^{-1}). For the experiments under different transmembrane pressure, R_m has been reported as function of pressure. The relative standard deviation in all measurements for flux was within the range of $\pm$ 13–19% and for filtration resistance was within the range of $\pm$ 4.6–13.7%. In the Supporting information Fig. S3 (a) and S3 (b), GPC chromatograms of the retentate and permeate from experiments with feed concentrations of 15 g/L lignin and 229 g/L DES, with 8.71 mL/s feed flowrate, and under the transmembrane pressure of 10 bar, are provided. As shown in Fig. S3 (a), there is no rejection for molecules with an apparent molecular weight below 200 g/mol, which includes the DES components lactic acid (90.08 g/mol) and choline chloride (139.62 g/mol). Fig. S3 (c) shows rejection as function of molecular weight for molecules with apparent molecular weight of 200 g/mol and above. The rejection increases as the molecular weight increases. Molecules with a molecular weight exceeding 2500 g/mol are subject to full rejection, with a rejection ratio of approximately 1. For molecules with a molecular weight range of 200–2500 g/mol, the rate of rejection goes above 0.40. In the subsequent section, we present the average lignin rejection, which was further integrated into the modeling procedure. The average lignin rejection was obtained using the ratios of peak areas of GPC chromatograms of the retentate and permeate samples and Eq 4. Using these ratios, the total integrated area was calculated presuming lignin to have a molecular weight of 200 g/mol and higher (Alvarez-Vasco et al., 2016). For the lignin rejection, the standard deviations have been shown in the plots. In the first subsection (↱3.1), experimental results are described and used as inputs for developing a model to estimate the system size of a large-scale, continuous UF-DF system. The modeling results are discussed in subsection 3.2.

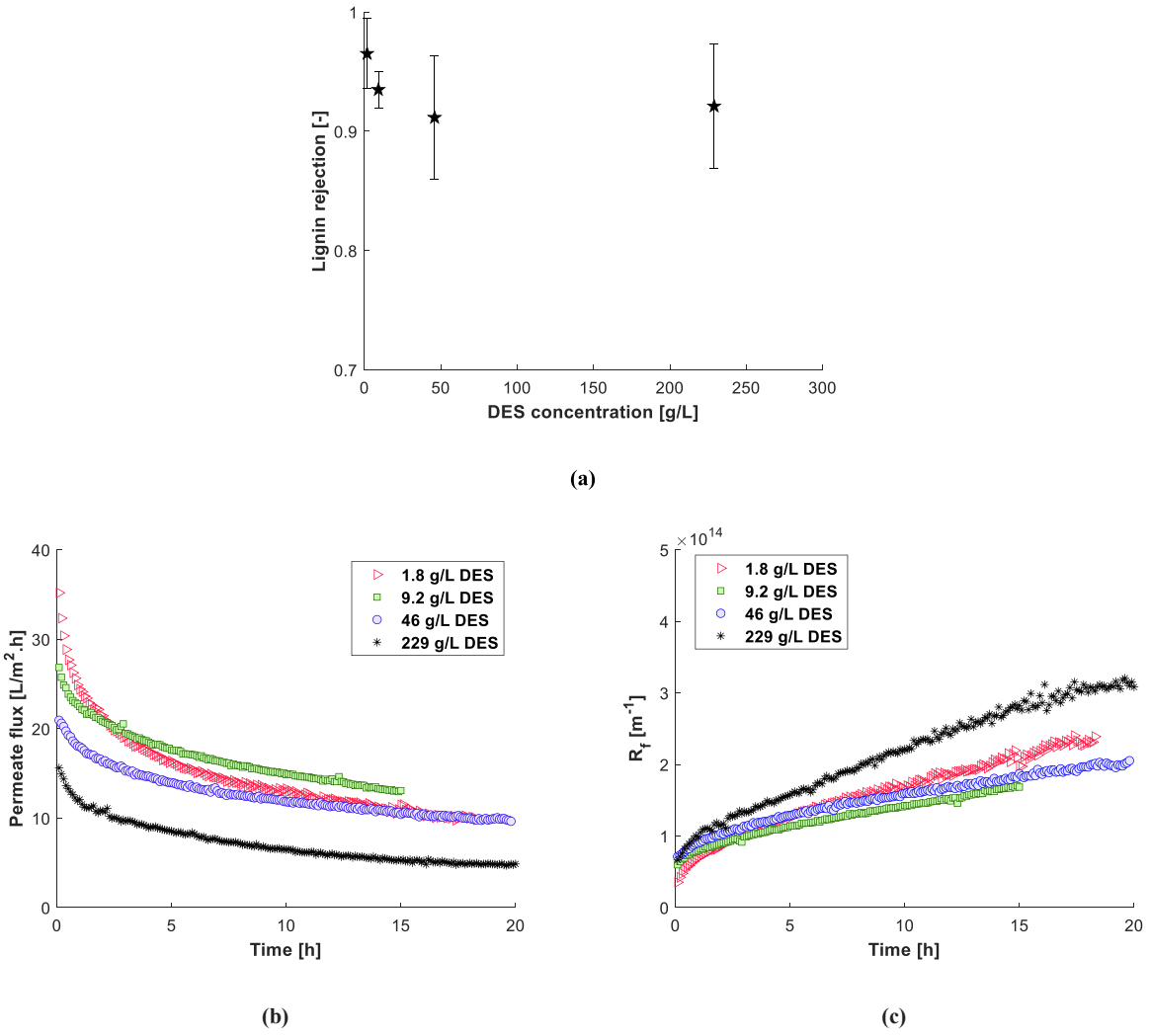

Fig. 5. Influence of different DES concentrations on: (a) lignin rejection, (b) flux decline and (c) filtration resistance, for a feed of 15 g/L lignin in acetone-water (70:30 v:v) with a feed flowrate of 8.71 mL/s, under the transmembrane pressure of 10 bar. The clean membrane resistance, R_m, is $4.42 \times 10^{13} \pm 13.7\%$ (m^{-1}) for all trials.

3.1. Experimental results

3.1.1. Influence of transmembrane pressure

To study the effect of transmembrane pressure on lignin rejection, flux decline, and filtration resistance, a feed of 15 g/L lignin and 229 g/L DES in the acetone-water (70:30 v:v) has been used at a feed flowrate of 8.71 mL/s. The results are displayed in Fig. 3.

From Fig. 3(a), there are no significant differences for lignin rejections with varying the pressures and always remains higher than 0.8. The pure solvent flux is seen to grow with pressure in Fig. 3(b). From Darcy's law Eq 2 rising pressure increases the driving forces that lead to a larger solvent flow (Saeid et al., 2023; van den Berg et al., 1989; Wijmans et al., 1984). It should be noted that the experiments conducted in this study were carried out without any prior compaction of the membrane. It was observed that the resistance of the clean membrane increases as the pressure increased up to 12 bar. This phenomenon can be attributed to the fact that higher pressure induces greater compaction within the membrane while using acetone-water, consequently affecting its performance (Stade et al., 2013). The acetone from the solvent could act as a plasticizer in the membrane matrix, allowing more compaction to take place compared to fully aqueous systems. Less membrane compaction at lower pressure allows the pores to effectively be larger, which has been described previously for ultrafiltration applications (Bhattacharya et al., 2005; Stade et al., 2013; Vinodhini and Sudha, 2016). In the Supporting information (Fig. S4 (a)) also demonstrated the solvent flux and membrane resistance across varying pressures for a pre-compacted membrane. Fig. S4 (b) illustrates the comparison between the pure water flux of a fresh pre-compacted membrane and the water flux of a membrane that has been flushed with solvent. The observed reduction in flux in the membrane that was flushed with the solvent indicates that the compaction of the membrane, which occurs during the solvent application, is likely to be irreversible. The time-dependent flux for the feed solution with 15 g/L lignin and 229 g/L DES at various pressures is depicted Fig. 3(c). The flux remains constant within the range of 2 to 8 bars, as observed variations fall within the experimental error margin of 13–19%. In this scenario, the increased pressure may not effectively reduce fouling and can potentially worsen fouling by pushing particles further into the membrane structure, thereby maintaining or decreasing the flux. As the applied pressure is further raised to 10 and 12 bar, the flux shows a slight initial increase as a result of the stronger driving forces. Nevertheless, as fouling increases, it ultimately returns to the same level observed at lower pressures. Fig. 3 (d) shows the filtration resistance over time for solution with 15 g/L lignin and 229 g/L DES at different pressures. The filtration resistance increases with increasing pressure up to 8 bar, after this point it appears to be constant. Since the flux remained constant for pressures less than 8 bar, the filtration resistance is proportional to pressure, and therefore, an increase in pressure causes an increase in filtration resistance (Eq 2)

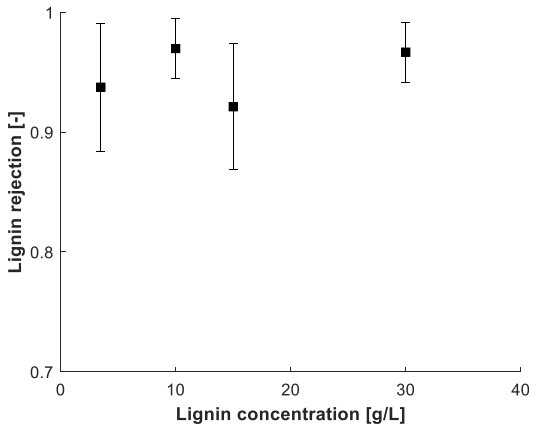

(a)

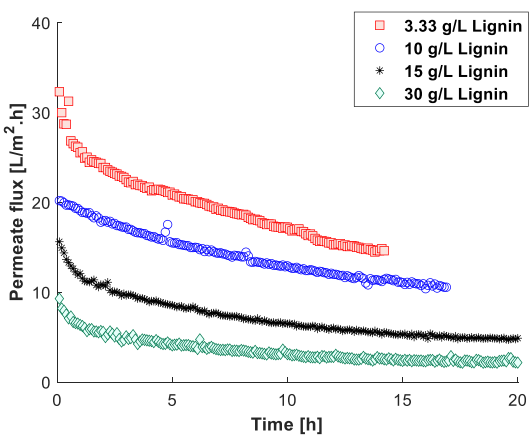

(b)

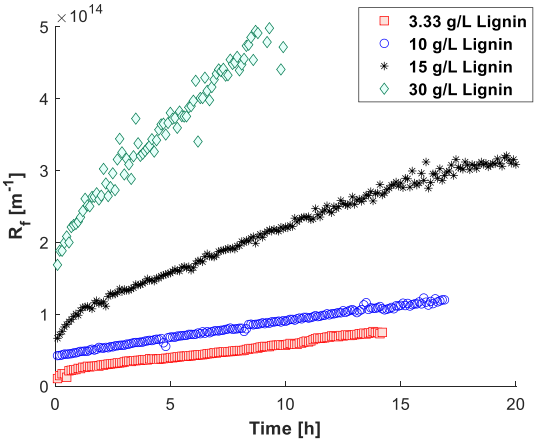

(c)

Fig. 6. Influence of different lignin concentrations on: (a) lignin rejection, (b) flux decline and (c) filtration resistance, for a feed of 229 g/L DES in acetone-water (70:30 v:v) with a feed flowrate of 8.71 mL/s, under the transmembrane pressure of 10 bar. The clean membrane resistance, R_m, is $4.42 \times 10^{13} \pm 13.7\%$ (m^{-1}) for all trials.

due to the more compaction of the cake layer on the surface of the membrane (Guo et al., 2012). For pressures of 8 bar and above, the filtration resistance is constant within the experimental error range (± 4.6–13.7%). Increasing the pressure from 5 to 8 bar and higher appears to increase the flux, which in turn causes higher drag forces (Bacchin et al., 2002; Guo et al., 2012), and higher lignin accumulation on the membrane's surface, leading to a sharper increase in filtration resistance over time. For pressures 8 to 12 bars however increasing the cake thickness matches the effect of increasing pressure or driving force, causing no significant changes in filtration resistance (Jiraratananon and Chanachai, 1996). For all pressures, the linear growth of the resistance curves after less than 1 h demonstrates that cake formation is the primary fouling mechanism at that time.

3.1.2. *Influence of feed flowrate*

The feed flowrate was adjusted to different flowrates, from 4.36 mL/s to 17.4 mL/s to examine the impact of the change on lignin rejection and filtration resistance due to lignin fouling. The results are displayed in Fig. 4.

Fig. 4(a) illustrates that lignin rejection for different feed flowrates. It appears that increasing the flowrate from 4.36 mL/s to 17.4 mL/s, in crossflow filtration has no significant influence on lignin rejections, and rejections are always above 0.9. Fig. 4(b) shows the flux decline along the membrane module for different feed flowrates. It can be seen that at increasing flowrate the flux is also higher. For the lower feed flowrates, a slightly sharper flux decline is observed at the beginning, which can be accounted for by higher pore-blocking and thicker CP layer at lower feed flowrate, also contributing to the higher overall filtration resistance (Fig. 4(c)) (Song, 1998; Wang and Song, 1999). At the initial flux decline zone, the higher turbulence at the higher flowrate causes particles on the surface of the membrane to diffuse back to the bulk, preventing them from reaching the membrane surface and resulting in less pore-blocking and thinner CP layer, as was previously also described by Ahmad et al., and Ikonić et al. (Ahmad et al., 2012; Ikonić et al., 2014). After the initial flux decline zone, the higher flowrates shear more of the accumulated lignin off the surface of the membrane, reducing the filtration resistance (Fig. 4(c)) thereby increasing the flux (Fig. 4(b)).

3.1.3. *Influence of DES concentration*

Considering that in an industrial continuous UF-DF process, the DES concentration will decrease over the course of the process due to addition of solvent in diafiltration, the impact of DES concentration on the flux and filtration resistance was experimentally evaluated (Gholami et al., 2022) by varying the DES concentration from 1.8 g/L to 229 g/L while the lignin content was held constant at 15 g/L. The selected DES concentrations are in the range that can be expected for a three-step

diafiltration process where 4 volumes of solvent are added per 1 volume unit of feed in each step. The pressure and flowrate were fixed at 10 bar and 8.71 mL/s for all trials. Fig. 5(a) depicts the lignin rejection, and it can be seen that the lignin rejection stays above 0.9 in all situations. While a slight decrease is seen while increasing the DES concentration, the trend is within the margins of the error bars. As can be seen in Fig. 5 (b), the initial flux increases by decreasing DES concentration from 229 g/L to 46 g/L and less, due to the lower feed solution's viscosity. In all the experiments presented, the initial permeate flux was not captured, and prior to the first data points, a noticeable decrease in permeate flux was already evident due to pore blocking and the development of a concentration polarization layer. However, the gradual decline in flux observed for DES concentrations of 46 g/L and lower (i.e., 9.2 g/L and 1.8 g/L) suggests that the rate of cake formation after the initial flux decline is dependent on lignin concentration, rather than DES concentration. It is worth noting that the lignin concentration is consistent across all feed solutions. In addition, increased DES concentration (greater lactic acid) induces de-swelling of the membrane matrix, resulting in smaller pores in the membrane and, therefore, lower flux, as similarly has been observed in the previous study (Gholami et al., 2022). The highest DES concentration leads to a more pronounced initial flux decline and lower flux in gradually flux decline zone. Fig. 5(c) shows changing in filtration resistance over time for different DES concentration. As is evident, DES concentrations below 229 g/L have a negligible impact on filtration resistance. However, the highest DES concentration results in a more sharp change in filtration resistance over time due to an increase in pore-blocking (Gholami et al., 2022), and consequently a greater cake growth rate over time.

3.1.4. Influence of lignin concentration

The influence of lignin concentration on lignin rejection, flux decline, and filtration resistance was investigated. To accomplish this, a number of feeds with varying lignin concentrations and a constant DES concentration of 229 g/L were utilized. Throughout all trials, the pressure and flow rate were held constant at 10 bar and 8.71 mL/s.

From Fig. 6(a), it can be seen that the lignin concentration does not have a significant impact of lignin rejection, it is always larger than 90%. Fig. 6(b) shows that the flux does decrease by increasing the lignin content. In all displayed experiments, the initial permeate flux was not captured, and before the first datapoints, already a significant permeate flux decline was observed (they all have the same permeate flux at time = 0). The higher the lignin content, the higher the flux decline. The resistance increases accordingly as is displayed in Fig. 6(c). Noting that the viscosity and density of the feed with different lignin concentrations are approximately the same (Gholami et al., 2022), the decrease in flux with increasing lignin concentration is due to the fact that in more concentrated solutions more molecules accumulate in and on the membrane (Lee and Clark, 1997), resulting in rapid pore-blocking in the initial stage and thicker cake layer on the surface of the membrane in the gradual flux decline zone. The filtration resistance (Fig. 6(c)) increase with increasing lignin content in the feed is due to the larger the cake deposition on the membrane's surface.

3.2. Modeling results

3.2.1. Flux decline model

After the rapid and often irreversible internal fouling of a membrane (Rawat et al., 2023), a cake layer is formed on the membrane surface, and the fouling due to this cake layer formation is reversible. The rate of the cake layer formation determines the back washing frequency for a membrane system. To describe the cake layer formation, a model was developed that models the growth of the fouling layer after the sharp decrease in flux observed initially in industrial scale UF-DF systems (Gholami et al., 2022). The model is based on gradual growth of the cake layer on the membrane surface over time to reach a constant thickness at steady state, which is the maximum cake thickness (Hidane et al., 2022).

Table 2
Fitted parameters using experimental data provided in section 3.1 at 10 bar.

Maximum thickness factor, K_1 $(m.L/g)$	1.9×10^{-2}
Cake growth coefficient, K_2 (L/g)	3.7×10^{-3}
Specific cake resistance, K_3 (m^{-2})	10.8×10^{16}

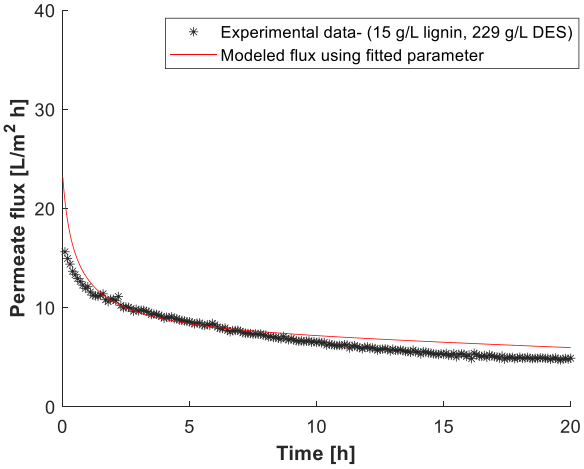

Fig. 7. Model fitted on experimental data for the feed with lignin concentration of 15 g/L and DES concentration of 229 g/L in a crossflow ultrafiltration measurements at 10 bar. With flowrate of 8.71 mL/s. (Solid line: modeled data using the fitted parameters presented in Table 2, symbols: experimental data).

The maximum thickness of the cake is a function of the Reynolds number (Hidane et al., 2022), and also dependent on lignin concentration, as lignin concentration affects the total mass contributing to cake formation and the thickness of the cake layer (Fig. 6).

The correlation for the maximum cake thickness, $\delta_{\max}$ (m), is given in Eq. 5:

$$\delta_{\max} = K_1 \frac{C_r}{\mathrm{Re}} \tag{5}$$

With K_1 being the maximum thickness factor $(m.\ L/g)$ and C_r the bulk lignin concentration in the feed (g/L) and Re is the Reynolds number. With this, the change in cake layer thickness can be calculated using following equation (Hidane et al., 2022; Nakamura and Matsumoto, 2006).

$$\frac{d\delta}{dt} = K_2 C_r J\left(1 - \frac{\delta}{\delta_{\max}}\right) \tag{6}$$

Where K_2 is the cake growth coefficient (L/g), J is the permeation flux $(m^3/m^2.s)$, and δ is the thickness of the cake layer (m) in time t. Until the thickness of the fouling layer reaches its steady state, this formula can be used (A.-S. Jönsson et al., 2008).

From Eq 2 and Eq 3, the permeation flux can be written as:

$$J = \frac{\Delta P}{\mu R_t} = \frac{\Delta P}{\mu (R_f + R_m)} \tag{7}$$

In this equation, R_f can be expressed as function of thickness of the cake layer (Dominiak et al., 2011; Endo and Alonso, 2001; Hidane et al., 2022).

$$R_f = K_3 \delta + R_{irr} \tag{8}$$

Where R_{irr} is the initial irreversible resistance (m^{-1}), which includes pore-blocking resistance but is insignificant compared to cake layer resistance (Ghaffour and Qamar, 2020; Khan et al., 2009) as evidenced by filtration resistance data in the experimental section 3.1. In order to facilitate calculations, constant values of 5×10^{13} and 4.42×10^{13}

Table 3
Parameters for modeling a full-scale continuous UF-DF process.

Channel height, H (m)	1.5×10^{-3}
Membrane width, W (m)	1
Applied pressure, ΔP_0 (Pa)	10^6
Initial lignin concentration, $C_{0,lignin}$ (g/L)	4.5
Initial DES concentration, $C_{0,DES}$ (g/L)	229
Initial feed velocity, u_{in} (m/s)	0.1
Lignin rejection (r)	0.90
Number of cells along the membrane channel	400
Clean membrane resistance, R_m (m^{-1})	4.42×10^{13}
Initial irreversible resistance, R_{irr} (m^{-1})	5×10^{13}
Number of pre-concentration modules	3
Number of diafiltration modules	3
Ratio of volume of added solvent to volume of initial feed for each diafiltration step	4

(m^{-1}) have been selected for R_{irr} and R_m, respectively, as the average values obtained from all experimental data collected under constant pressure conditions. K_3 is the specific cake resistance (m^{-2}), which is assumed to be constant during the constant pressure filtration process (Ghaffour and Qamar, 2020).

3.2.2. Fitting the parameters

Eqs. 5–8 were solved simultaneously using the forward Euler method in MATLAB (version R2022a) by iterating over time to obtain K_1, K_2 and K_3 via fitting to the experimental data reported in section 3.1 for 10 bar (Table 2).

An example of flux prediction using the fitted parameters on experimental data has been shown in Fig. 7. The remaining fitting plots for various lignin and DES concentrations and flowrates are available in the Supporting information S5. The relative root mean squared error (RRMSE) for the fitting parameters for all experimental data is in the range of 0.025 and 0.34.

3.2.3. Prediction of a large scale UF-DF system

This section describes a modified version of the model developed in our previous study for designing a UF-DF system at an industrial scale based on the experimental results in the crossflow setup. A flat-sheet membrane configuration, was considered for modeling (Gholami et al., 2022). A schematic description of the membrane feed channel considered for each module is available in Supporting information S6. The model was numerically solved using MATLAB (version R2022a) and the algorithm is shown in Supporting information S7. The membrane channel was split into at least 400 cells for all of the simulations in this study Noting that the previously developed model was based on dead-end results. Here, we propose a modified model that employs the flux model described in section 3.2, allowing for a more precise estimation of system size.

In addition to the fitted values for the parameters given in Table 2, the remaining model parameters are listed in Table 3. Each diafiltration stage requires an additional solvent equal to four times the volume of feed solution entering that stage; this excess solvent is recoverable by evaporation or membrane separation. Based on the experimental data provided in section 3.1, the clean membrane resistance (R_m), the initial irreversible resistance (R_{irr}) and lignin rejection (r) has been considered 4.42×10^{13}, 5×10^{13} and 0.90, respectively.

A scheme of the continuous UF-DF membrane system used in the model is shown in Fig. 8. The model allows for variation of the number of modules for both pre-concentration and diafiltration. In this case the number of module for both steps is set to 3. In the pre-concentration the lignin concentration is increased from 4.5 to 30 g/L. This value is chosen to be similar to an earlier study (Gholami et al., 2022) and it is based on the DES-based delignification process design by Smink et al. (Smink et al., 2020c). The selected initial feed velocity (0.1 m/s) and membrane channel size (Table 3), suggest a system with an initial feed flowrate of 540 L/h treating 2.43 Kg/h lignin. The lignin concentration of the retentate stream coming out from the pre-concentration, is 30 g/L and the DES concentration is still 229 g/L. The membrane is assumed unselective for DES as has been shown in the experimental results as well

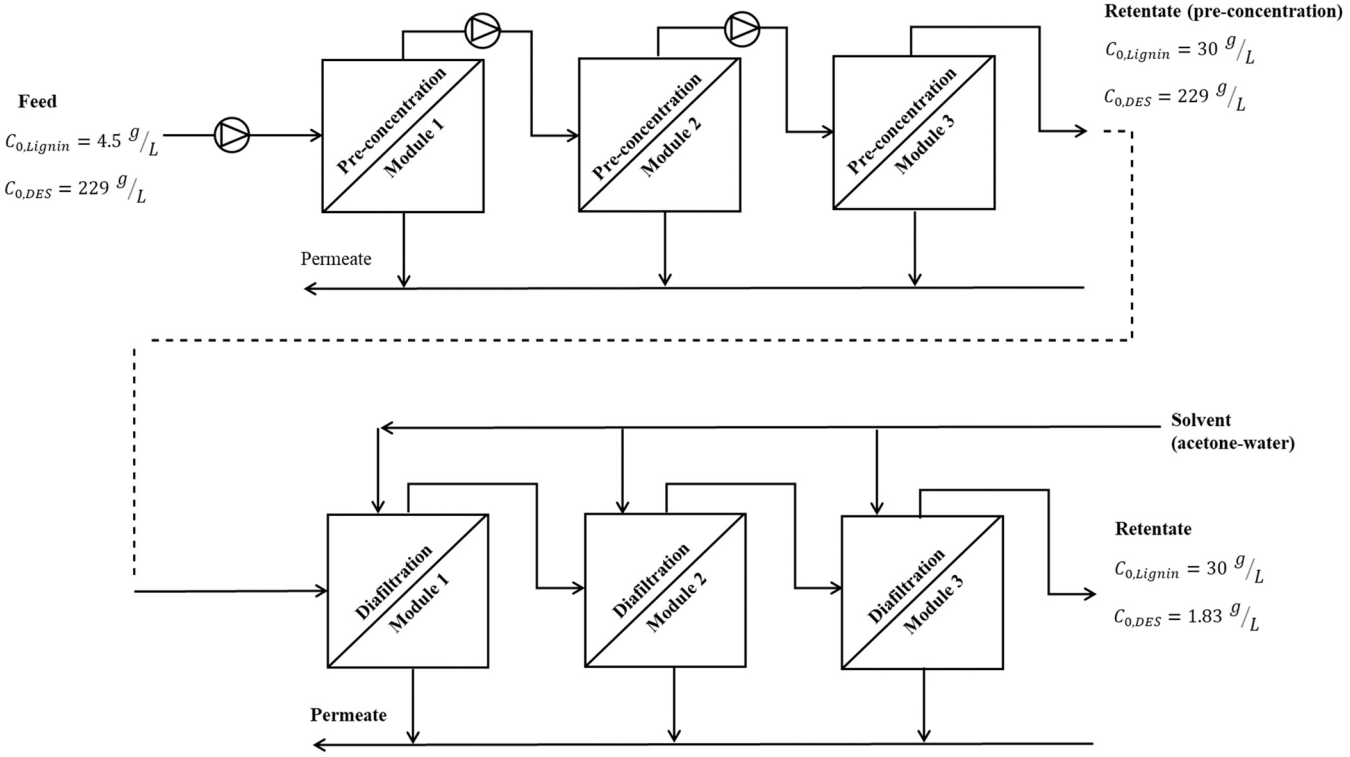

Fig. 8. Continuous UF-DF considered for the modeling.

Table 4
Mathematical formulation for transmembrane pressure calculation along the feed channel (Gholami et al., 2022).

Transmembrane pressure along the feed channel (Pa)	$(\Delta P^i)_t = (\Delta P^{i-1})_t - (\Delta P_{loss})_t$	(9)
Friction coefficient (-)	$f = \frac{6.23}{\mathrm{Re}^{0.3}}$	(10)
Pressure drop along the feed channel (Pa)	$(\Delta P_{loss})_t = \frac{f}{2}\frac{l}{h}\rho(u^i)_t^2$	(11)

(Supporting information, S3). Next this feed is diluted by a factor 5 to 45.8 g/L of DES and 6 g/L lignin. Then in the first diafiltration module the lignin concentration increases up to 30 g/L again. This is repeated in modules 2 and 3. This results in a retentate stream of 1.83 g/L DES and 30 g/L lignin, which has been considered to be the solubility limit of lignin in the solvent. Hence, there is no need to have the post-concentration.

The flux decline in a large-scale continuous UF-DF system was predicted using the method used in our earlier work (Gholami et al., 2022) coupled with the flux decline model described in section 3.2. For this, K_1, K_2, and K_3 are considered to be constant throughout all modules at the 10 bar fixed pressure. Noting that the pressure loss throughout each membrane module is negligible, the fitted parameters can be utilized as an input value when modeling the large scale UF-DF to determine the filtration resistance and flux in each stage.

The transmembrane pressure in any location of i and time t, has been calculated using Eqs 9–11 as has been explained in previous study (Gholami et al., 2022).(Table 4).

Viscosity (μ) and density (ρ) of the permeate has been assumed to be dependent on DES concentration and is calculated using data provided in the previous study (Gholami et al., 2022). Solving the lignin mass balance along the length of the module at location i and time t gives the following expression for the lignin concentration:

$$(C_r^i)_t = \left(\frac{C_r^{i-1}V_r^{i-1} - (1-r)C_r^{i-1}J^{i-1}a}{V_r^i}\right)_t \quad (12)$$

In this equation, a is the cell surface area measured by dividing the channel membrane area by the number of cells. V_r refers to the volume flowrate in the retentate side at location i and time t. and r is the rejection of lignin.

3.2.4. Lignin concentration profile and required membrane area

In the Fig. 9(a) and (b) the concentration profile for lignin over the length of each membrane module for modeled UF-DF system over a time of 2 days has been shown. From these results, the required length for membrane module increases over time by increasing the cake layer and filtration resistance against the flux. However, for pre-concentration a length of less than 80 m seems to be enough for each module to let the system work for 2 days without back-washing. The required length for diafiltration modules is increasing since by adding solvent in this stage the volume entering the system is increasing. However, the required

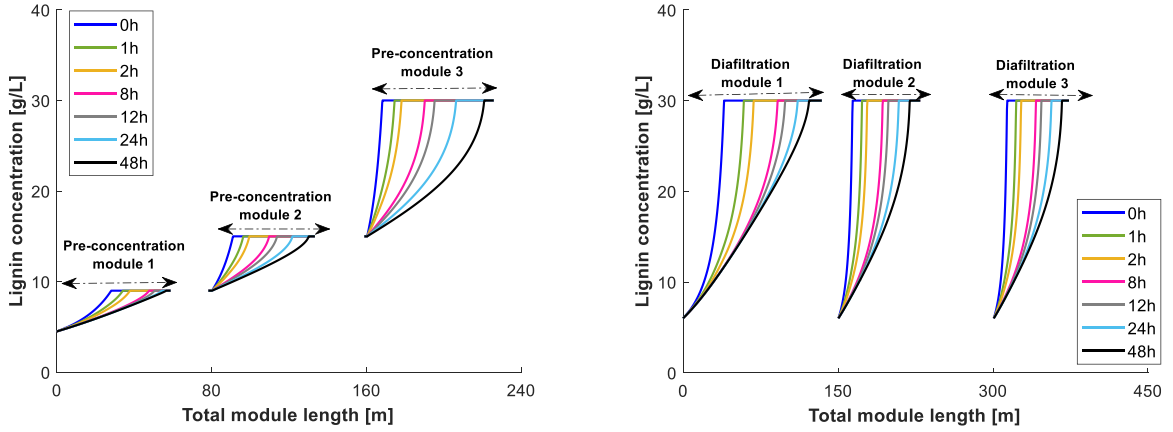

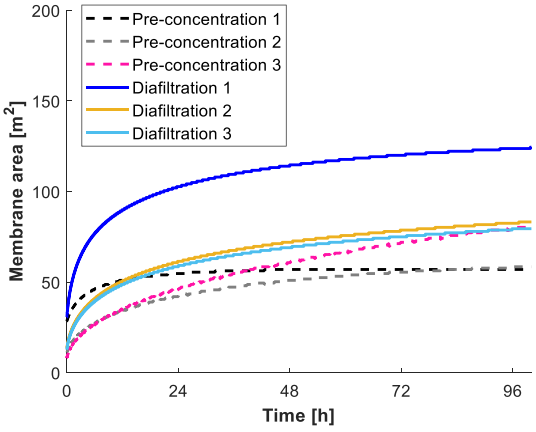

Fig. 9. Lignin concentration along the membrane channel for each module of modeled UF-DF system as described in Fig. 8. (a) Pre-concentration (b) Diafiltration and (c) Required area of each membrane module as function of time.

membrane size for diafiltrations 2 and 3 is smaller than for diafiltration 1, as DES concentration decreases, resulting in increased flux. Fig. 9(c) shows the required area in each module increases over time as the fouling causes a lower flux, resulting in a larger membrane area needed. Considering these results, do a back-washing every 8 h or less to remove the cake layer and reduce the resistance seems to be reasonable, otherwise the maximum of 422 m^2 membrane is required to allow UF-DF system works for longer than 3 days.

The given modeling study showed that a continuous UF-DF system is an effective separation and purification technique for lignin recovery from DES-black liquor. Since fouling is still a significant issue for UF separation, the back-washing frequency and needed membrane surface area must be chosen sensibly. Future research should aim to create a precise estimate of the energy required for lignin recovery from the retentate stream. Notably, using a solvent-resistant membrane for the current application may increase the permeation flux while simultaneously enhancing lignin rejection, thereby reducing the size of the membrane system required.

4. Conclusions

Under various operational conditions, the flux decline and fouling behavior of a crossflow ultrafiltration process for the separation and purification of lignin from DES-black liquid following delignification of biomass were studied. Under all operational conditions, lignin has a consistently high rejection (average of 0.90). Consistently achieving high rejection can be attributed to factors such as lignin molecule size, lignin's back diffusion, pore blocking and cake formation on the surface of the membrane, These factors prevent lignin passing through the membrane. Membrane compaction under increasing pressure can alter the behavior of pore-blocking and subsequent cake development on the membrane's surface. The lower the lignin concentration, the higher the flux and the lower the filtration resistance. It was also discovered that DES concentrations 46 g/L and lower have a minimal effect on filtration resistance. However, the highest DES concentration causes a more severe change in filtration resistance over time due to an increase in pore-blocking. Due to the decreased viscosity of the feed solution, the initial flux rises as DES content decreases. In addition, increasing DES concentration (more lactic acid) stimulates de-swelling of the membrane polymer, resulting in smaller pores in the membrane and thus increased pore-blocking.

In order to obtain constant parameters of maximum thickness factor, cake growth coefficient, and specific cake resistance, the filtration flux was evaluated and fitted to experimental data for various feed concentrations and flowrates. Then, these parameters were used to predict flux decrease and filtration resistance in the large-scale UF-DF process. The results of the modeling showed that lignin in DES-black liquor could be separated and purified from the other molecules by using acetone-water as the solvent in a continuous UF-DF system with three stages of pre-concentration and three stages of diafiltration. As a cake layer forms on the membrane's surface, the total area needed by each module rises. Yet, the size of such a system can be selected to be reduced by having a back-washing in an acceptable frequency. It is important to determine how much energy is required to separate the lignin in the retentate stream and the solvent in the permeate stream so that both can be reused.

Future research could focus on conducting a comprehensive experimental study to investigate a wider range of operating conditions. Finding the ideal condition for this process that minimizes fouling and maximizes flux would be the goal. Furthermore, the actual DES-black liquor is a complex mixture containing not only lignin and DES but also hemicellulose, its derivatives, and trace minerals which can impact the efficiency of this separation method in real life. Future research should include employing UF filtration with real DES-black liquor to investigate the impact of the presence of such impurities in of the filtration process.

CRediT authorship contribution statement

Mahsa Gholami: Investigation, methodology, data analysis, writing - original draft. Bram Middelkamp: Investigation, methodology, data analysis. Yagnaseni Roy: Conceptualization, Supervision, Review & editing, Methodology. Wiebe M. de Vos: Supervision, Review & editing, Methodology. Boelo Schuur: Supervision, project administration, funding acquisition, writing – review & editing, methodology.

Declaration of Competing Interest

The authors declare no conflict of interest.

Acknowledgment

This project is called PRIDES and is co-funded by the Institute for Sustainable Process Technology (ISPT) and TKI E&I with the supplementary grant 'TKI-Toeslag' for Topconsortia for Knowledge and Innovation (TKI's) of the Ministry of Economic Affairs and Climate Policy. The authors would like to thank all members of the ISPT Consortium for their contribution. The consortium consists of the following organizations: BASF, CTP, CTST, Mayr-Melnhof, Mid Sweden University, Mondi, Sappi, Stora Enso, University of Aveiro, University of Twente, Valmet, VTT, WEPA and Zellstof Pöls. More information can be found on https://ispt.eu/programs/deep-eutectic-solvents/.

Appendix A. Supporting information

Supplementary data associated with this article can be found in the online version at doi:10.1016/j.cherd.2024.01.013.

References

Ahmad, A.L., Mat Yasin, N.H., Derek, C.J.C., Lim, J.K., 2012. Crossflow microfiltration of microalgae biomass for biofuel production. Desalination 302, 65–70. https://doi.org/10.1016/j.desal.2012.06.026.

Alvarez-Vasco, C., Ma, R., Quintero, M., Guo, M., Geleynse, S., Ramasamy, K.K., Wolcott, M., Zhang, X., 2016. Unique low-molecular-weight lignin with high purity extracted from wood by Deep Eutectic Solvents (DES): a source of lignin for valorization. Green. Chem. 18, 5133–5141. https://doi.org/10.1039/C6GC01007E.

Arni, S.Al, 2018. Extraction and isolation methods for lignin separation from sugarcane bagasse: a review. Ind. Crops Prod. 115, 330–339. https://doi.org/10.1016/j.indcrop.2018.02.012.

Bacchin, P., Si-Hassen, D., Starov, V., Clifton, M.J., Aimar, P., 2002. A unifying model for concentration polarization, gel-layer formation and particle deposition in cross-flow membrane filtration of colloidal suspensions. Chem. Eng. Sci. 57, 77–91. https://doi.org/10.1016/S0009-2509(01)00316-5.

Bhattacharya, P.K., Todi, R.K., Tiwari, M., Bhattacharjee, C., Bhattacharjee, S., Datta, S., 2005. Studies on ultrafiltration of spent sulfite liquor using various membranes for the recovery of lignosulphonates. Desalination 174, 287–297. https://doi.org/10.1016/j.desal.2004.09.017.

Chovau, S., Degrauwe, D., Van der Bruggen, B., 2013. Critical analysis of techno-economic estimates for the production cost of lignocellulosic bio-ethanol. Renew. Sustain. Energy Rev. 26, 307–321. https://doi.org/10.1016/j.rser.2013.05.064.

da Costa Lopes, A.M., Gomes, J.R.B., Coutinho, J.A.P., Silvestre, A.J.D., 2020. Novel insights into biomass delignification with acidic deep eutectic solvents: a mechanistic study of β-O-4 ether bond cleavage and the role of the halide counterion in the catalytic performance. Green. Chem. 22, 2474–2487. https://doi.org/10.1039/C9GC02569C.

Deuss, P.J., Scott, M., Tran, F., Westwood, N.J., de Vries, J.G., Barta, K., 2015. Aromatic monomers by in situ conversion of reactive intermediates in the acid-catalyzed depolymerization of lignin. J. Am. Chem. Soc. 137, 7456–7467. https://doi.org/10.1021/jacs.5b03693.

Domínguez-Robles, J., Tamminen, T., Liitiä, T., Peresin, M.S., Rodríguez, A., Jääskeläinen, A.-S., 2018. Aqueous acetone fractionation of kraft, organosolv and soda lignins. Int J. Biol. Macromol. 106, 979–987. https://doi.org/10.1016/j.ijbiomac.2017.08.102.

Dominiak, D., Christensen, M., Keiding, K., Nielsen, P.H., 2011. Gravity drainage of activated sludge: new experimental method and considerations of settling velocity, specific cake resistance and cake compressibility. Water Res. 45, 1941–1950. https://doi.org/10.1016/j.watres.2010.12.029.

Du, X., Zhang, K., Yang, H., Li, K., Liu, X., Wang, Z., Zhou, Q., Li, G., Liang, H., 2019. The relationship between size-segregated particles migration phenomenon and combined

membrane fouling in ultrafiltration processes: the significance of shear stress. J. Taiwan Inst. Chem. Eng. 96, 45–52. https://doi.org/10.1016/j.jtice.2018.11.016.
Endo, Y., Alonso, Manuel, 2001. Physical meaning of specific cake resistance and effects of cake properties in compressible cake filtration. Filtr. Sep. 38, 42–46. https://doi.org/10.1016/S0015-1882(01)80447-X.
Fernández-Rodríguez, J., Erdocia, X., Hernández-Ramos, F., Alriols, M.G., Labid, J., 2018. Lignin separation and fractionation by ultrafiltration. Sep. Funct. Mol. Food Membr. Technol. 229–265. https://doi.org/10.1016/B978-0-12-815056-6.00007-3.
Ghaffour, N., Qamar, A., 2020. Membrane fouling quantification by specific cake resistance and flux enhancement using helical cleaners. Sep Purif. Technol. 239, 116587 https://doi.org/10.1016/j.seppur.2020.116587.
Gholami, M., Schuur, B., Roy, Y., 2022. Ultrafiltration-based diafiltration for post-delignification fractionation of lignin from a deep eutectic solvent comprised of lactic acid and choline chloride. Sep Purif. Technol., 122097 https://doi.org/10.1016/j.seppur.2022.122097.
Gholami, M., Tijburg, J.M., Schuur, B., 2023. Comparing organic solvents in a combined water precipitation and liquid–liquid extraction process to recover lignin and furanics from a lactic acid: choline chloride deep eutectic solvent used as cooking liquor for cooking of spruce. Biomass Convers. Biorefin. https://doi.org/10.1007/s13399-023-04580-4.
Guo, W., Ngo, H.-H., Li, J., 2012. A mini-review on membrane fouling. Bioresour. Technol. 122, 27–34. https://doi.org/10.1016/j.biortech.2012.04.089.
Hidane, T., Demura, M., Morisada, S., Ohto, K., Kawakita, H., 2022. Mathematical analysis of cake layer formation in an ultrafiltration membrane of a phycobiliprotein-containing solution extracted from Nostoc commune. Biochem Eng. J. 179, 108333 https://doi.org/10.1016/j.bej.2022.108333.
Holtz, A., Weidener, D., Leitner, W., Klose, H., Grande, P.M., Jupke, A., 2020. Process development for separation of lignin from OrganoCat lignocellulose fractionation using antisolvent precipitation. Sep Purif. Technol. 236, 116295 https://doi.org/10.1016/j.seppur.2019.116295.
Ikonić, B.B., Takači, A.A., Zavargo, Z.Z., Šereš, Z.N., Šaranović, Ž.V., Ikonić, P.M., 2014. Fuzzy modeling of the permeate flux decline during microfiltration of starch suspensions. Chem. Eng. Technol. 37, 709–716. https://doi.org/10.1002/ceat.201300550.
Ippolitov, V., Anugwom, ikenna, Deun, R., Mänttäri, M., Kallioinen-Mänttäri, M., 2022. Cellulose membranes in the treatment of spent deep eutectic solvent used in the recovery of lignin from lignocellulosic biomass. Membranes 12, 86. https://doi.org/10.3390/membranes12010086.
Jablonsky, M., Majova, V., Skulcova, A., Haz, A., 2018. Delignification of pulp using deep eutectic solvents. J. Hyg. Eng. Des. 22, 76–81.
Jiraratananon, R., Chanachai, A., 1996. A study of fouling in the ultrafiltration of passion fruit juice. J. Memb. Sci. 111, 39–48. https://doi.org/10.1016/0376-7388(95)00270-7.
Jönsson, A.S., Nordin, A.K., Wallberg, O., 2008. Concentration and purification of lignin in hardwood kraft pulping liquor by ultrafiltration and nanofiltration. Chem. Eng. Res. Des. 86, 1271–1280. https://doi.org/10.1016/J.CHERD.2008.06.003.
Jönsson, A.-S., Nordin, A.-K., Wallberg, O., 2008. Concentration and purification of lignin in hardwood kraft pulping liquor by ultrafiltration and nanofiltration. Chem. Eng. Res. Des. 86, 1271–1280. https://doi.org/10.1016/j.cherd.2008.06.003.
Khan, S.J., Visvanathan, C., Jegatheesan, V., 2009. Prediction of membrane fouling in MBR systems using empirically estimated specific cake resistance. Bioresour. Technol. 100, 6133–6136. https://doi.org/10.1016/j.biortech.2009.06.037.
Lee, Y., Clark, M.M., 1997. A numerical model of steady-state permeate flux during cross-flow ultrafiltration. Desalination 109, 241–251. https://doi.org/10.1016/S0011-9164(97)00070-2.
Li, P., Cheng, X., Zhou, W., Luo, C., Tan, F., Ren, Z., Zheng, L., Zhu, X., Wu, D., 2020. Application of sodium percarbonate activated with Fe(II) for mitigating ultrafiltration membrane fouling by natural organic matter in drinking water treatment. J. Clean. Prod. 269, 122228 https://doi.org/10.1016/j.jclepro.2020.122228.
Li, T., Lyu, G., Liu, Y., Lou, R., Lucia, L.A., Yang, G., Chen, J., Saeed, H.A.M., 2017. Deep eutectic solvents (DESs) for the isolation of willow lignin (Salix matsudana cv. zhuliu). Int J. Mol. Sci. 18 https://doi.org/10.3390/ijms18112266.
Lipnizki, F., 2010. Chapter 7 - Membrane processes for the production of bulk fermentation products. In: Cui, Z.F., Muralidhara, H.S. (Eds.), Membrane Technology. Butterworth-Heinemann, Oxford, pp. 121–153. https://doi.org/10.1016/B978-1-85617-632-3.00007-0.
Liu, Y., Deak, N., Wang, Z., Yu, H., Hameleers, L., Jurak, E., Deuss, P.J., Barta, K., 2021. Tunable and functional deep eutectic solvents for lignocellulose valorization. Nat. Commun. 12, 5424 https://doi.org/10.1038/s41467-021-25117-1.
Madsen, R.F., 2001. Design of sanitary and sterile UF- and diafiltration plants. Sep Purif. Technol. 22–23, 79–87. https://doi.org/10.1016/S1383-5866(00)00144-1.
Morya, R., Kumar, M., Tyagi, I., Kumar Pandey, A., Park, J., Raj, T., Sirohi, R., Kumar, V., Kim, S.-H., 2022. Recent advances in black liquor valorization. Bioresour. Technol. 350, 126916 https://doi.org/10.1016/j.biortech.2022.126916.
Nakamura, K., Matsumoto, K., 2006. Properties of protein adsorption onto pore surface during microfiltration: effects of solution environment and membrane hydrophobicity. J. Memb. Sci. 280, 363–374. https://doi.org/10.1016/j.memsci.2006.01.039.
Pang, T., Wang, G., Sun, H., Sui, W., Si, C., 2021. Lignin fractionation: effective strategy to reduce molecule weight dependent heterogeneity for upgraded lignin valorization. Ind. Crops Prod. 165, 113442 https://doi.org/10.1016/j.indcrop.2021.113442.
Pérez, A.D., Fiskari, J., Schuur, B., 2021. Delignification of low-energy mechanical pulp (Asplund Fibers) in a deep eutectic solvent system of choline chloride and lactic acid, 0, 418 Front Chem.. https://doi.org/10.3389/FCHEM.2021.688291.
Putro, J., Soetaredjo, F., Lin, S.-Y., Ju, Y.-H., Ismadji, S., 2016. Pretreatment and conversion of lignocellulose biomass into valuable chemicals. RSC Adv. 6 https://doi.org/10.1039/C6RA09851G.
Rawat, S., Chaudhary, M., Maiti, A., 2023. Synergistic arsenic removal using chitosan-based nanocomposite beads and cross-flow ultrafiltration: a significant reduction of membrane fouling. J. Environ. Chem. Eng. 11, 109431 https://doi.org/10.1016/j.jece.2023.109431.
Roy, Y., Top, R.W., de Vos, W.M., Schuur, B., 2023. Organic solvent reverse osmosis (OSRO) for the recovery of hemicellulosic derivatives after wood-pulping with a deep eutectic solvent. Chem. Eng. Sci. 267, 118367 https://doi.org/10.1016/j.ces.2022.118367.
Saeid, P., Zeinolabedini, M., Khamforoush, M., 2023. Simulation of a crossflow ultrafiltration polysulfone/polyvinylpyrrolidone membrane separation using finite element analysis to separate oil/water emulsion. Iran. Polym. J. 32, 447–455. https://doi.org/10.1007/s13726-022-01134-9.
Schuur, B., Brouwer, T., Smink, D., Sprakel, L.M.J., 2019. Green solvents for sustainable separation processes. Curr. Opin. Green. Sustain Chem. 18, 57–65. https://doi.org/10.1016/j.cogsc.2018.12.009.
Servaes, K., Varhimo, A., Dubreuil, M., Bulut, M., Vandezande, P., Siika-aho, M., Sirviö, J., Kruus, K., Porto-Carrero, W., Bongers, B., 2017. Purification and concentration of lignin from the spent liquor of the alkaline oxidation of woody biomass through membrane separation technology. Ind. Crops Prod. 106, 86–96. https://doi.org/10.1016/j.indcrop.2016.10.005.
Smink, D., Juan, A., Schuur, B., Kersten, S.R.A., 2019. Understanding the role of choline chloride in deep eutectic solvents used for biomass delignification. Ind. Eng. Chem. Res. 58, 16348–16357. https://doi.org/10.1021/acs.iecr.9b03588.
Smink, D., Kersten, S.R.A., Schuur, B., 2020a. Comparing multistage liquid–liquid extraction with cold water precipitation for improvement of lignin recovery from deep eutectic solvents. Sep Purif. Technol. 252, 117395 https://doi.org/10.1016/j.seppur.2020.117395.
Smink, D., Kersten, S.R.A., Schuur, B., 2020b. Recovery of lignin from deep eutectic solvents by liquid-liquid extraction. Sep Purif. Technol. 235, 116127 https://doi.org/10.1016/j.seppur.2019.116127.
Smink, D., Kersten, S.R.A., Schuur, B., 2020c. Process development for biomass delignification using deep eutectic solvents. Conceptual design supported by experiments. Chem. Eng. Res. Des. 164, 86–101. https://doi.org/10.1016/j.cherd.2020.09.018.
Song, L., 1998. Flux decline in crossflow microfiltration and ultrafiltration: mechanisms and modeling of membrane fouling. J. Memb. Sci. 139, 183–200. https://doi.org/10.1016/S0376-7388(97)00263-9.
Stade, S., Kallioinen, M., Mikkola, A., Tuuva, T., Mänttäri, M., 2013. Reversible and irreversible compaction of ultrafiltration membranes. Sep Purif. Technol. 118, 127–134. https://doi.org/10.1016/j.seppur.2013.06.039.
Stoner, M.R., Fischer, N., Nixon, L., Buckel, S., Benke, M., Austin, F., Randolph, T.W., Kendrick, B.S., 2004. Protein−solute interactions affect the outcome of ultrafiltration/diafiltration operations. J. Pharm. Sci. 93, 2332–2342. https://doi.org/10.1002/jps.20145.
Sun, Z., Fridrich, B., de Santi, A., Elangovan, S., Barta, K., 2018. Bright side of lignin depolymerization: toward new platform chemicals. Chem. Rev. 118, 614–678. https://doi.org/10.1021/acs.chemrev.7b00588.
Tan, Y., Chua, A., Ngoh, G., 2020. Deep eutectic solvent for lignocellulosic biomass fractionation and the subsequent conversion to bio-based products – a review. Bioresour. Technol. 297 https://doi.org/10.1016/j.biortech.2019.122522.
Tanistra, I., Bodzek, M., 1998. Preparation of high-purity sulphate lignin from spent black liquor using ultrafiltration and diafiltration processes. Desalination 115, 111–120. https://doi.org/10.1016/S0011-9164(98)00030-7.
Toledano, A., García, A., Mondragon, I., Labidi, J., 2010. Lignin separation and fractionation by ultrafiltration. Sep Purif. Technol. 71, 38–43. https://doi.org/10.1016/J.SEPPUR.2009.10.024.
van den Berg, G.B., Rácz, I.G., Smolders, C.A., 1989. Mass transfer coefficients in cross-flow ultrafiltration. J. Memb. Sci. 47, 25–51. https://doi.org/10.1016/S0376-7388(00)80858-3.
Vinodhini, P.A., Sudha, P.N., 2016. Removal of heavy metal chromium from tannery effluent using ultrafiltration membrane. Text. Cloth. Sustain. 2, 5 https://doi.org/10.1186/s40689-016-0016-3.
Wang, L., Song, L., 1999. Flux decline in crossflow microfiltration and ultrafiltration: experimental verification of fouling dynamics. J. Memb. Sci. 160, 41–50. https://doi.org/10.1016/S0376-7388(99)00075-7.
Wang, N., Li, X., Yang, Y., Zhou, Z., Shang, Y., Zhuang, X., 2020. Photocatalysis-coagulation to control ultrafiltration membrane fouling caused by natural organic matter. J. Clean. Prod. 265, 121790 https://doi.org/10.1016/j.jclepro.2020.121790.
Wang, Z., Liu, Y., Barta, K., Deuss, P.J., 2022. The effect of acidic ternary deep eutectic solvent treatment on native lignin. ACS Sustain Chem. Eng. 10, 12569–12579. https://doi.org/10.1021/acssuschemeng.2c02954.
Wijmans, J.G., Nakao, S., Smolders, C.A., 1984. Flux limitation in ultrafiltration: osmotic pressure model and gel layer model. J. Memb. Sci. 20, 115–124. https://doi.org/10.1016/S0376-7388(00)81327-7.
Xu, J., Li, C., Dai, L., Xu, C., Zhong, Y., Yu, F., Si, C., 2020. Biomass fractionation and lignin fractionation towards lignin valorization. ChemSusChem 13, 4284–4295. https://doi.org/10.1002/cssc.202001491.
Zijlstra, D.S., Lahive, C.W., Analbers, C.A., Figueirêdo, M.B., Wang, Z., Lancefield, C.S., Deuss, P.J., 2020. Mild organosolv lignin extraction with alcohols: the importance of benzylic alkoxylation. ACS Sustain Chem. Eng. 8, 5119–5131. https://doi.org/10.1021/acssuschemeng.9b07222.